Advances in Long Wavelength Interband Cascade Lasers

J. A. Massengale[1,2*], Yixuan Shen[1], R. Q. Yang[1], S. D. Hawkins[3], and J. F. Klem[3]

[1]*School of Electrical and Computer Engineering, University of Oklahoma, Norman, OK 73019, USA*
[2]*Homer L. Dodge Department of Physics and Astronomy, University of Oklahoma, Norman, OK 73019, USA*
[3]*Sandia National Laboratories, PO Box 5800, Albuquerque, NM, 87185-1085 USA*

*Email: massengalej@ou.edu

Abstract – We demonstrate significantly improved performance of InAs-based interband cascade lasers (ICLs) operating in extended wavelength regions covering 10-13 μm with threshold current densities (J_{th}) as low as 12 A/cm^2 and continuous-wave (cw) output powers greater than 40 mW/facet.

I. Introduction

Interband cascade lasers (ICLs) [1] utilize the type-II broken gap alignment in III-V materials, along with a cascade configuration, to achieve efficient lasing operation in the mid-infrared wavelength region with low power consumption [2-3]. While ICLs based on type-II quantum well (QW) active regions have demonstrated excellent performance in the 3 – 6 μm range [2-3], extension to longer wavelengths is challenging due to several factors, including reduced wavefunction overlap in the type-II QW and higher free-carrier absorption loss. Another concern is the significant increase of the thickness of the optical cladding layers needed to accommodate the longer optical wave decay length. Traditionally, InAs/AlSb superlattices (SLs) are used as the cladding layers, which complicates molecular beam epitaxy (MBE) growth. Such SLs have a low thermal conductivity and so an increase in the overall SL thickness causes the thermal resistance of the device to increase accordingly, hindering performance [2-6]. For the InAs-based ICL, a combination of an undoped InAs separate confinement layer (SCL), InAs/AlSb SL intermediate cladding layer, and n^+-InAs plasmon cladding layer have been shown to improve the performance at longer wavelengths [7]. Additionally, the operating wavelength can be extended to greater than 13 μm by altering the configuration of the QW active region to include $InAs_{0.5}P_{0.5}$ barriers, which lowers the interband transition energy [8]. In our previous work, there were some uncertainties in the expected operating wavelength for devices with such a modified QW active region, which chiefly manifested in high internal absorption losses, leading to relatively large threshold current densities (J_{th}) and low external quantum efficiencies (EQE) and output powers. For this work, four 20-stage ICLs were grown, two with the advanced waveguide and two with both the advanced waveguide and the $InAs_{0.5}P_{0.5}$ barriers in the QW active region. To accommodate the longer wavelength emission, the waveguide layer thicknesses were slightly increased by about 18%, 5%, and 7% for the InAs SCL, InAs/AlSb SL intermediate, and n^+-InAs plasmon cladding layers, respectively. Also, the doping concentration in the InAs plasmon cladding was reduced by about 13%, doping in the injection region reduced by about 31%, and the InAs layer thicknesses in the QW active region were slightly adjusted.

II. Results

Broad-area (100- and 150-μm-wide and 1.5-mm-long) ICL devices were fabricated, with multiple devices operating across the four wafers as shown in Fig. 1, which indicates a reduction of the J_{th} and increase of operating temperatures compared to previous ICLs at similar wavelengths [7]. ICLs with only the advanced waveguide, EB7541BA3-1D, were able to operate in both cw and pulsed modes with a J_{th} of 12 A/cm^2 at 80 K, representing about a 50% reduction compared to previous ICLs operating at similar wavelengths. These ICLs were able to operate in cw mode up to 123 K and up to 153 K in pulsed mode near 11 μm, with a maximum cw output power at 80 K of over 40 mW/facet, more than 3 times as much as our previous ICL [7] as shown in Fig. 2. The extracted EQE under cw operation reached ~532% at 80 K, indicating the cascaded emission of photons in the ICL, and dropped to ~ 97% at 120 K as shown in Fig. 2. Compared to our previous devices, the cw threshold voltage V_{th} (4.82 V at 80 K) was substantially reduced, by ~ 50%. ICLs with both the advanced waveguide and the inclusion of the $InAs_{0.5}P_{0.5}$ barriers in the QW active region, EB7523BA3-1F, exhibited similarly improved performance in the longer wavelength region (12-13 μm). In contrast to our previously reported ICL, devices made from this wafer had reduced J_{th} and were able to operate in both cw and pulsed modes, though heating was a major limiting factor for cw performance as the J_{th} required for lasing in this longer wavelength region is larger compared to ICLs near 11 μm as shown in Fig. 1. Nevertheless, the J_{th} was ~ 59% lower than previous devices at similar wavelengths [7] which employed $InAs_{0.5}P_{0.5}$ barriers. The output power was more than 3 times larger and the extracted EQE at 80 K was improved by more than 5 times (212% vs 41%) as shown in Fig. 4. The lasing wavelengths from wafers EB7539 and EB7547, which have slightly thick InAs layer thicknesses in QW active regions, are somewhat longer than that from EB7523 and EB7541, respectively. These results indicate that the structural changes made have improved the carrier transport and reduced the internal absorption losses that were previously present. We anticipate further improvements can be made.

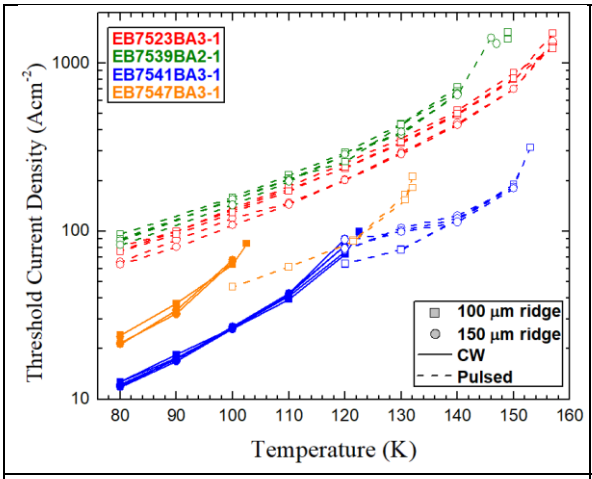

Fig. 1. Threshold current density (J_{th}) as a function of temperature for several devices made from the four recent ICL wafers.

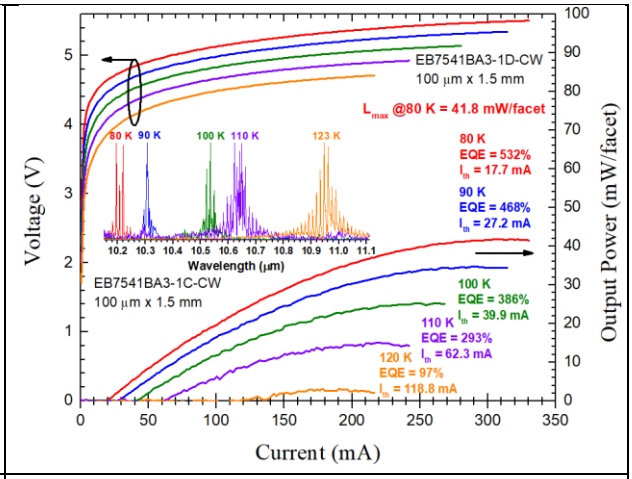

Fig. 2. Current-voltage-power (IVL) characteristics for EB7541BA3-1D in cw mode. The inset shows the cw emission spectra of EB7541BA3-1C between 80 K and 123 K.

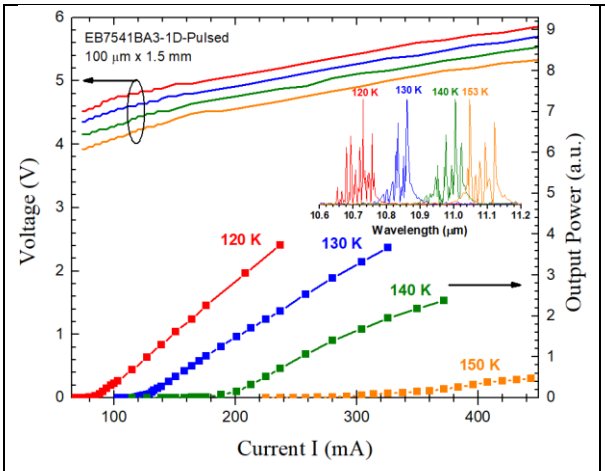

Fig. 3. Current-voltage-power (IVL) characteristics for EB7541BA3-1D in pulsed mode. The inset shows the pulsed emission spectra between 120 K and 153 K.

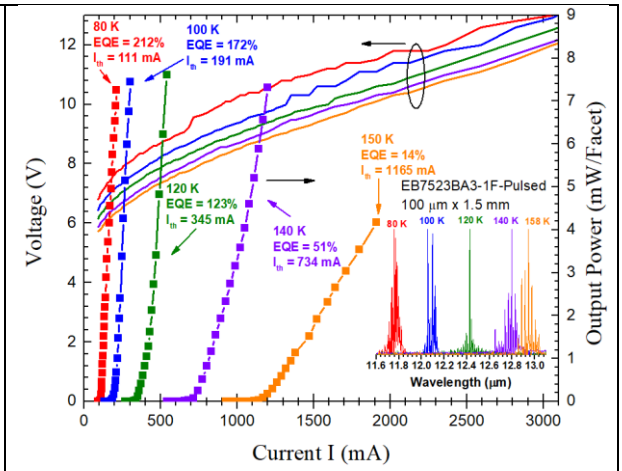

Fig. 4. Current-voltage-power (IVL) characteristics for EB7523BA3-1F in pulsed mode. The inset shows the pulsed emission spectra between 80 K and 158 K.

Acknowledgement: The work at the University of Oklahoma was partially supported by NSF (ECCS-1931193). This work was performed, in part, at the Center for Integrated Nanotechnologies, an Office of Science User Facility operated for the U.S. Department of Energy (DOE) Office of Science. SNL is managed and operated by NTESS under DOE NNSA contract DE-NA0003525.

III. References

[1] R. Q. Yang, "*Infrared laser based on intersubband transitions in quantum wells",* Superlattices Microstruct., **17**, 77 (1995).
[2] J. R. Meyer, *et al*, *"The interband cascade laser",* Photonics, **7**, 75 (2020).
[3] R. Q. Yang, *et al*, "*InAs-based interband cascade lasers",* IEEE J. Sel. Top. Quant. Electron., **25**, 1200108 (2019).
[4] M. Dallner, F Hau, S Höfling, M Kamp, "InAs-based interband cascade lasers emitting around 7 μm with threshold current densities below 1 kA/cm^2 at room temperature", Appl. Phys. Lett., **106**, 041108 (2015).
[5] L. Li, *et al*, "*Low-threshold InAs-based interband cascade lasers operating at high temperatures",* Appl. Phys. Lett., **106**, 251102 (2015).
[6] Lu Li, *et al*, *"MBE-grown long-wavelength interband cascade lasers on InAs substrates",* Journal of Crystal Growth, **425**, 369 (2015).
[7] J. A. Massengale, Y. Shen, R. Q. Yang, S. D. Hawkins, and J. F. Klem, "*Long wavelength interband cascade lasers*," Appl. Phys. Lett. **120**, 091105 (2022).
[8] R. Q. Yang, "Electronic states and interband tunneling conditions in type-II quantum well heterostructures," J. Appl. Phys. **127**, 025705 (2020).